

Machine learning continuous-variable quantum key distribution embedded with quantum multi-label classifier

Qin Liao,^{1,*} Hai Zhong,² and Ying Guo^{3,†}

¹*College of Computer Science and Electronic Engineering, Hunan University, Changsha 410082, China*

²*School of Computer Science and Engineering, Central South University, Changsha 410083, China*

³*School of Automation, Central South University, Changsha 410083, China*

(Dated: June 13, 2022)

We propose a brand-new protocol called machine learning continuous-variable quantum key distribution (ML-CVQKD), aiming to break the limitation of traditional pattern in CVQKD and establish a cross research platform between CVQKD and machine learning. ML-CVQKD divides the whole system into state learning process and state prediction process. The former is used for training and estimating quantum classifier, and the latter is used for predicting unlabeled signal states. Meanwhile, a quantum multi-label classification (QMLC) algorithm is designed as an embedded classifier for ML-CVQKD. Feature extraction for coherent state and machine learning-based criteria for CVQKD are successively suggested. QMLC-embedded ML-CVQKD protocol could improve the performance of CVQKD system in terms of both secret key rate and transmission distance, and it provides a novel approach for improving the practical CVQKD system.

PACS numbers: 42.50.St

I. INTRODUCTION

For decades, continuous-variable quantum key distribution (CVQKD) [1, 2] has been a hotspot in quantum communication and quantum cryptography. It provides an approach to allows two distant legitimate partners, Alice and Bob, to share a random secure key over insecure quantum and classical channels.

One of the advantage of CVQKD protocols comparing its discrete-variable quantum key distribution (DVQKD) [3, 4] counterpart is that the most state-of-art telecommunication technologies can be compatible to CVQKD protocols, so that one may apply CVQKD system to the practical communication network in use. Moreover, CVQKD protocols have been shown to be secure against arbitrary collective attacks, which are optimal in both the asymptotic limit [5–8] and the finite-size regime [9, 10]. Recently, CVQKD is further proved to be secure against collective attacks in composable security framework [11], which is the security analysis by carefully considering every detailed step in CVQKD system.

In general, there are two modulation approaches in CVQKD protocol, i.e., Gaussian modulated CVQKD protocol [12, 13] and discretely modulated CVQKD protocol [14–17]. For the first approach, Alice usually encodes key bits in the quadratures (\hat{p} and \hat{q}) of optical field [18], while Bob can restore the secret key bits through high-speed and high-efficiency coherent detection techniques. This strategy usually has a repetition rate higher than that of single-photon detections so that Gaussian modulated CVQKD could potentially achieve higher secret key rate. However, it seems unfortunately limited to much shorter distance due to the problem of

quite low reconciliation efficiency in long-distance transmission. For the other approach, it generates several nonorthogonal coherent states and exploits the sign of the measured quadrature of each state to encode information rather than using the quadrature \hat{p} or \hat{q} itself. This discrete modulation strategy is more suitable for long-distance transmission since the sign of the measured quadrature is already discrete, thereby validating most excellent error-correcting codes even at low SNR.

However, most of the existing CVQKD protocols, whether Gaussian modulated protocols or discretely modulated protocols, are based on communication-related techniques, and comply with the similar pattern in which raw key is firstly generated and followed by the post-processing including reconciliation, parameter estimation, error-correcting and privacy amplification [19]. These nearly identical procedures with a variety of communication-related techniques of CVQKD protocols have been investigated for a dozen years. Although a number of excellent CVQKD protocols have been proposed such as measurement-device-independent (MDI) CVQKD protocols [20–24], plug-and-play (PP) CVQKD protocols [25, 26], unidimensional CVQKD protocols [27–29], entangled-source-in-middle (ESIM) CVQKD protocols [30, 31], phase-encoded and basis-encoded CVQKD protocols [32, 33] etc., one may hardly make a further breakthrough for CVQKD due to the limitation of its traditional pattern and techniques.

In recent years, machine learning (ML) [34] has been widely applied and has shown its powerful impact upon diverse research fields such as artificial intelligence, image processing, data mining and so on. However, few researches about applying machine learning to CVQKD has been conducted except some preliminary studies [35, 36]. To break the limitation of traditional pattern and establish a cross research platform between CVQKD and machine learning, in this paper, we suggest a special-

* llqqlq@hnu.edu.cn

† yingguo@csu.edu.cn

ized framework for performing continuous-variable quantum key distribution. By introducing machine learning methodology, we redesign the whole process of CVQKD system, called machine learning CVQKD (ML-CVQKD), making it more suitable for the various machine learning implementations. In particular, the process of ML-CVQKD contains all possible steps for supervised learning algorithms [37] involving training, testing and prediction, each step of which is vital for classifying the received coherent state. ML-CVQKD waives the necessity of error correction and parameter estimation during post-processing so that one can exploit more raw key to generate the final secret key. In the meantime, a well-behaved quantum multi-label classification (QMLC) algorithm is proposed as an embedded classifier. This specially designed quantum classifier is not only quite suitable for the ML-CVQKD system, but also beneficial for the performance improvement of CVQKD. The quality of the whole system can be simultaneously assessed by a single machine learning parameter so that the complicated estimation of covariance matrix of quantum system is no longer required. Moreover, the proposed protocol can be applied to the existing system without deploying any extra equipment. We show that the proposed QMLC-embedded ML-CVQKD protocol can improve the performance of CVQKD system with tolerable low error rate. The size of data block used for generating positive secret key is much less so that ML-CVQKD is much more suitable for real-time transmission.

This paper is structured as follows. In Sec. II, we demonstrate the proposed machine learning CVQKD system, namely ML-CVQKD. In Sec. III, we elaborate the principle of embedded QMLC algorithm. Performance analysis are discussed in Sec. IV and final conclusions are drawn in Sec. V.

II. MACHINE LEARNING CVQKD SYSTEM

In this section, we first briefly retrospect the traditional process of CVQKD system, and then give the detailed description of the specialized framework, ML-CVQKD.

A. Traditional process of CVQKD

Since F. Grosshans and P. Grangier put forward the initial Gaussian modulated coherent state (GG02) protocol [38], scholars have proposed plenty of improved schemes. Subsequently, A. Leverrier et al. further modified the process by taking finite-size effect into account [39], rendering the traditional process become a standard for most CVQKD systems.

As can be seen from Fig. 1(b), the prepare-and-measurement (PM) process for traditional CVQKD system is composed of following steps [11].

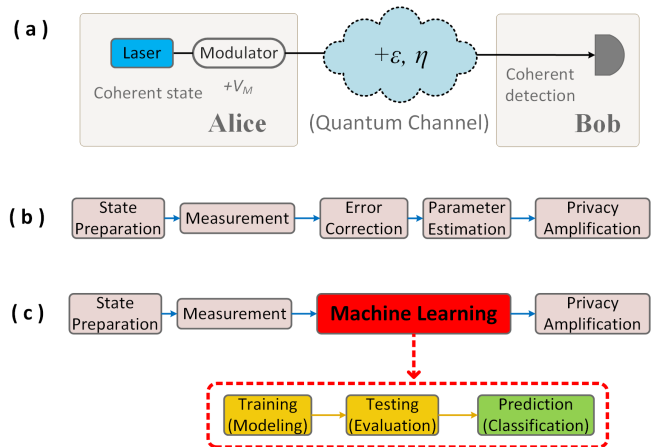


FIG. 1. (a) Schematic diagram of prepare-and-measurement CVQKD protocol. (b) The process for traditional CVQKD protocol. (c) ML-CVQKD in which steps of error correction and parameter estimation are substituted by machine learning process.

State Preparation Alice first prepares a modulated coherent state, and sends it to Bob through an untrusted quantum channel.

Measurement Bob then measures the incoming state with coherent detection so that Alice and Bob share two correlated sets variables, i.e. raw key.

Error Correction One first needs to discretize the yielded raw key if Gaussian modulation is used, and then a linear error correcting code, usually a low density parity check (LDPC) code [40], is exploited to automatically reconcile the data between Alice and Bob.

Parameter Estimation Bob sends a part of bits of information to Alice that allow her to infer the characteristic of the quantum channel and compute the covariance matrix of quantum system.

Privacy Amplification Alice and Bob apply a random hash function to their respective strings so that they can obtain two identical strings, i.e., secret key.

The above process is based on information theory, so that one needs to correct the erroneous code and evaluate the quality of quantum channel, which makes error correction and parameter estimation become the most crucial steps in traditional CVQKD protocol. However, a part of resources such as the generated raw key, storage and computing of devices have to be inevitably sacrificed for these two steps. To break the limitation and reduce the cost, ML-CVQKD is suggested in what follows.

B. Process of ML-CVQKD

As shown in Fig. 1(c), it depicts that parts of traditional CVQKD process are replaced by machine learning. The classic machine learning, especially supervised learning, involves three modules, i.e., training, testing and prediction. Each module is responsible for respective task,

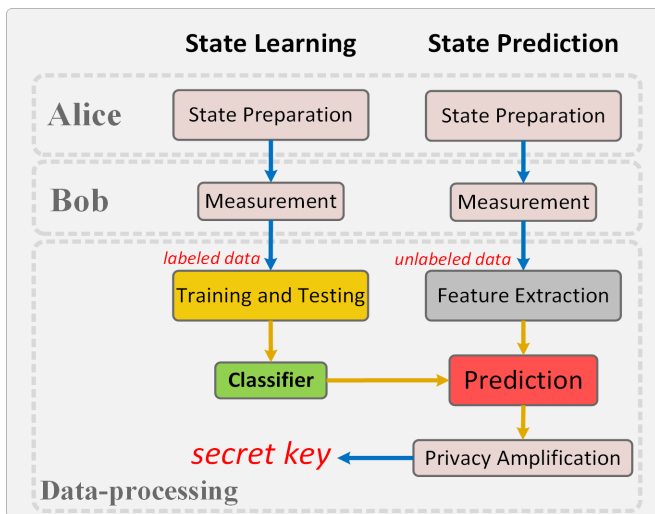


FIG. 2. The framework for machine learning CVQKD process. It is composed of two parts, state learning for modeling and evaluation, and state prediction for classification.

i.e. modeling, evaluation and classification. Specifically, to construct the classifier, a training set is first used for learning the classification rules. Subsequently, another set of data, called testing set, is exploited to evaluate the classifier’s performance. Finally, the trained classifier can be used for predicting unknown data if the evaluation is passed. Inspired by the classic machine learning process, we design a framework for ML-CVQKD process which includes two parts. As shown in Fig. 2, we now explain each step as follows.

State Learning

Step 1 Alice first prepares labeled coherent states, and sends them to Bob through untrusted quantum channel.

Step 2 Bob measures the incoming states with coherent detector thereby obtains the measurement results. Note that these results are similar to, but not identical to the modulated information sent by Alice, this is because the transmitted signals are inevitably distorted by several negative effects such as channel noise and loss.

Step 3 After collecting sufficient data, Bob divides them into two datasets, i.e. training set and testing set. The former is used for training classifier, and the latter is used to evaluate the classifier’s performance and the quality of quantum channel.

Step 4 A well-behaved quantum classifier for ML-CVQKD is prepared if testing is passed.

Once the classifier has been trained successfully, one does not need to perform state learning repeatedly.

State Prediction

Step 1 Alice prepares modulated coherent states and sends them to Bob through untrusted quantum channel.

Step 2 Bob obtains the measurement results (unlabeled) by measuring the received states with coherent detector.

Step 3 Bob first extracts features from the obtained unknown data, these features are subsequently used as

input data for the prepared classifier.

Step 4 Bob classifies the input data using the well-behaved classifier, so that he can predict the state that Alice sent to him. After many rounds of prediction, Alice and Bob share a string of key.

Step 5 To further enhance the security, Alice and Bob apply a random hash function to their respective strings. Finally, they respectively obtain two identical strings, i.e. secret key.

The proposed ML-CVQKD process is quite different with traditional CVQKD. Due to the framework is designed for various machine learning algorithms so that a learning process (state learning) is necessary for training the classifier. Error correction and parameter estimation are no longer required for ML-CVQKD since their duties can be integrated into state learning. Once the classifier is prepared, all data can be used for generating secret key rather than sacrifice part of it for error correcting and parameter estimation, resulting in the performance improvement of CVQKD. Furthermore, the data-processing of ML-CVQKD does not need any extra device or component so that it is convenient to apply existing machine learning algorithms to enhance the practical CVQKD system.

III. QUANTUM CLASSIFIER FOR ML-CVQKD

As known, lots of classification algorithms have proposed for solving traditional classifier problems, such as Decision Tree, Neural Network, Support Vector Machine (SVM) and so on. However, few algorithms are suggested for classifying quantum state. To enhance the performance of CVQKD system, we propose a quantum multi-label classification (QMLC) algorithm for ML-CVQKD.

QMLC is derived from a traditional lazy learning approach called k -nearest neighbor (k NN) [41]. It selects k nearest neighbors for each unknown data point. Based on the number of neighboring data belonging to each possible class, maximum a posteriori (MAP) principle can be exploited to allocate the label to the unknown data point. Fig. 3 depicts an example of k NN approach in feature space. The green circle denotes an unknown data point, while triangles and rectangles represent the labeled data points which respectively belong to red class and yellow class. The green circle will be assigned to the red class for $k = 3$, since two of the 3-nearest labeled data points belong to the red class while only one point belongs to the yellow class. Similarly, the green circle will be labeled as yellow class for $k = 7$.

k NN classifies unknown data in feature space which enlightens us that coherent states can probably be classified in its phase space. As shown in Fig. 4(a), the phase space is divided into several regions, which are labeled as L_i ($i = 1, 2, 3, 4$) according to their located quadrant. We find that each QPSK-modulated coherent state belongs to a single label, which can be deemed quantum single-label learning depicted in Fig. 4(c). How-

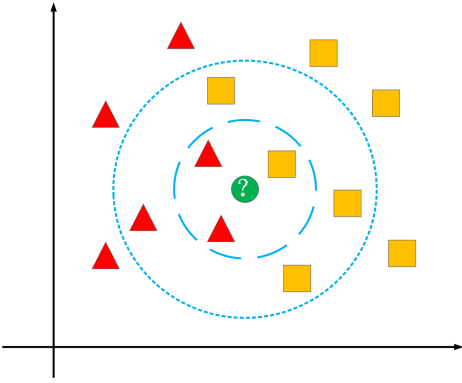


FIG. 3. The k -nearest neighbor classification algorithm in feature space. Green circle denotes an unknown data point, triangles and rectangles belong to red class and yellow class, respectively. Blue dashed circle represents $k = 3$ while blue dotted circle represents $k = 7$.

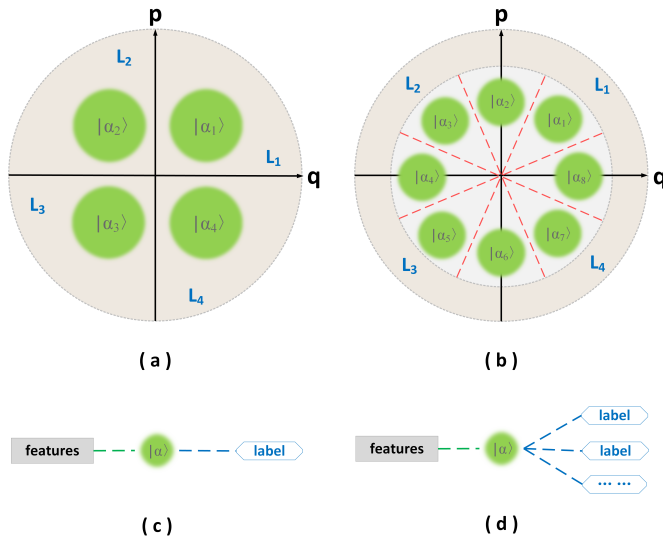


FIG. 4. (Top) Phase space representation of coherent states with (a) QPSK and (b) 8PSK modulation. Each coherent state is assigned only one label in QPSK or multiple (at least one) labels in 8PSK. (Bottom) Quantum machine learning model for (c) single-label learning and (d) multi-label learning.

ever, with the development of modulation technique, 8PSK [42], 16PSK and even quadrature amplitude modulation (QAM) [43] are applied to further improve the performance of CVQKD system. As an example, Fig. 4(b) shows the phase space representation of coherent states with 8PSK modulation. Thereinto, some of 8PSK-modulated coherent states, such as $|\alpha_2\rangle$, $|\alpha_4\rangle$, $|\alpha_6\rangle$ and $|\alpha_8\rangle$, simultaneously belong to multiple labels, which can be generalized into quantum multi-label learning in Fig. 4(d).

In fact, single label is a special case of multiple labels, so that both can be described by the model of multi-

label learning. In what follows, we detail the proposed QMLC algorithm for addressing the generalized multi-label CVQKD model. Without loss of generality, we consider the algorithm for the 8PSK-modulated CVQKD since it is the simplest multi-label modulation scheme. We note that the proposed QMLC algorithm can also be extended for other complicated modulation schemes.

A. Feature extraction for coherent state

As known, feature extraction is an important data-preprocessing step in machine learning, since a set of suitable features would significantly enhance classification performance. The more features are extracted, the more details about the object can be obtained. However, there is few apparent features to describe a modulated coherent state, except for a few attributes such as p -quadrature, q -quadrature and modulated variance V_M .

To solve the above-mentioned problem, we construct a set of distance features for each coherent state. As shown in Fig. 5, Alice sends a modulated coherent state through an untrusted quantum channel (usually a single mode fiber, SMF), and then the transmitted coherent state is received by Bob. Note that the transmitted state is no longer identical with its initial modulated state due to the phase drift ($\theta' \neq \theta$) and energy attenuation ($\sqrt{p'^2 + q'^2} < \sqrt{p^2 + q^2}$) caused by the imperfect channel noise and loss. Subsequently, a number of virtual states (we named them reference states) are set for calculating the similarities of the transmitted state and reference states. In particular, the similarity can be measured by *Euclidean metric*, which is the straight-line distance between two points in Euclidean space [44]. In the Cartesian coordinates, we assume $\mathbf{y} = (y_1, y_2, \dots, y_n)$ and $\mathbf{z} = (z_1, z_2, \dots, z_n)$ are two points in Euclidean n -dimensional space, and the distance d between \mathbf{y} and \mathbf{z} is given by

$$d(\mathbf{y}, \mathbf{z}) = \sqrt{\sum_{i=1}^n (y_i - z_i)^2}. \quad (1)$$

Specifically, in the 2-dimensional phase space we have

$$d_w(\mathbf{t}, \mathbf{r}) = \sqrt{(p' - p_{r_w})^2 + (q' - q_{r_w})^2}, \quad (2)$$

where w is the number of reference state, $\mathbf{t} = (p', q')$ and $\mathbf{r} = (p_r, q_r)$ are the respective Cartesian points of transmitted state and r -th reference state. After that, we can extract a set of feature vectors $\mathbf{d} = (d_1, d_2, \dots, d_w)$ for better description of the transmitted states.

As mentioned above, reference states are a set of virtual states that do not really exist, and hence one does not need to prepare them at Bob's side. In general, reference states are set to be identical with initial modulated states, which can help us to investigate the influence of imperfect channel on transmitted state.

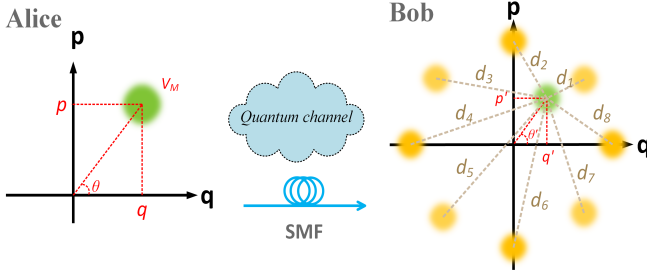


FIG. 5. Feature extraction of 8PSK-modulated coherent state. (Left) Alice sends the modulated coherent state through the noisy and lossy channel. (Right) Bob receives the transmitted coherent state and extracts its distance features. Green dot denotes signal state, and yellow dot denotes virtual state, i.e. reference state.

B. Quantum multi-label classifier

After extracting robust features, these features are subsequently used as input data of classifier for state learning. Assuming $\mathcal{X} = \mathbb{R}^d$ is d -dimensional data space, and $\mathcal{Y} = \{y_1, y_2, \dots, y_l\}$ is label space containing l categories. A training set is given by $\mathcal{D} = \{(\mathbf{x}_i, Y_i) | 1 \leq i \leq m\}$, where $\mathbf{x}_i \in \mathcal{X}$ is d -dimensional attribute vector $(x_{i1}, x_{i2}, \dots, x_{id})^T$ and $Y_i \subseteq \mathcal{Y}$ is a set of labels to which \mathbf{x}_i belongs. The task of learning system is to find a multi-label classifier $h(\cdot) : \mathcal{X} \rightarrow 2^{\mathcal{Y}}$. Namely, for a given threshold function $t : \mathcal{X} \rightarrow \mathbb{R}$, it renders $h(\mathbf{x}) = \{y | f(\mathbf{x}, y) > t(\mathbf{x}), y \in \mathcal{Y}\}$.

Let $|x\rangle$ be an unlabeled coherent state, and $\mathcal{N}(|x\rangle)$ denotes the subset of k nearest coherent states of $|x\rangle$ in training set. The following statistic will be calculated as

$$C_j = \sum_{(|x^*>, Y^*) \in \mathcal{N}(|x\rangle)} \mathbb{I}[y_j \in Y^*], \quad (3)$$

where C_j counts the number of neighbors of $|x\rangle$ belonging to the j -th category y_j ($1 \leq j \leq l$). Assuming H_j represents the event that coherent state $|x\rangle$ has label y_j , then $\mathbb{P}(H_j | C_j)$ denotes the posteriori probability, where H_j is true under the condition that C_j is the labeled data in $\mathcal{N}(|x\rangle)$ have label y_j . Accordingly, $\mathbb{P}(\bar{H}_j | C_j)$ denotes the posteriori probability which H_j is false under the condition that C_j labeled data in $\mathcal{N}(|x\rangle)$ with label y_j . Let $f(|\mathbf{x}\rangle, y_j) = \mathbb{P}(H_j | C_j) / \mathbb{P}(\bar{H}_j | C_j)$, the quantum multi-label classifier can be expressed by

$$h(|\mathbf{x}\rangle) = \{y_j | \mathbb{P}(H_j | C_j) / \mathbb{P}(\bar{H}_j | C_j) > t(|\mathbf{x}\rangle), 1 \leq j \leq l\}. \quad (4)$$

In other words, unlabeled coherent state $|x\rangle$ can be assigned to category y_j when posteriori probability $\mathbb{P}(H_j | C_j)$ is greater than $t(|x\rangle) \cdot \mathbb{P}(\bar{H}_j | C_j)$.

Specifically, based on *Bayesian theorem* [35], function $f(|\mathbf{x}\rangle, y_j)$ can be rewritten as

$$f(|\mathbf{x}\rangle, y_j) = \frac{\mathbb{P}(H_j | C_j)}{\mathbb{P}(\bar{H}_j | C_j)} = \frac{\mathbb{P}(H_j) \cdot \mathbb{P}(C_j | H_j)}{\mathbb{P}(\bar{H}_j) \cdot \mathbb{P}(C_j | \bar{H}_j)}, \quad (5)$$

where $\mathbb{P}(H_j)$ and $\mathbb{P}(\bar{H}_j)$ respectively represent the prior probability that event H_j is true or false, $\mathbb{P}(C_j | H_j)$ and $\mathbb{P}(C_j | \bar{H}_j)$ respectively represent the conditional probability of C_j labeled coherent states in $\mathcal{N}(|x\rangle)$ with label y_j under the condition that event H_j is true or false.

The probabilities in Eq. (5) can be estimated by frequency counting in training set. In particular, prior probabilities can be calculated by

$$\mathbb{P}(H_j) = \frac{s + \sum_{i=1}^m \mathbb{I}[y_j \in Y_i]}{s \times 2 + m} \quad (1 \leq j \leq l), \quad (6)$$

and

$$\mathbb{P}(\bar{H}_j) = 1 - \mathbb{P}(H_j) \quad (1 \leq j \leq l), \quad (7)$$

where s is a smoothing parameter controlling the weight of uniform prior distribution during probability estimates, and it usually set to 1 for *Laplace smoothing*.

Different from prior probability, the estimation of conditional probabilities in Eq. (5) is complicated. For the j -th category y_j ($1 \leq j \leq l$), we calculate two arrays ς_j and $\bar{\varsigma}_j$, each of which contains $k + 1$ elements given by

$$\varsigma_j[r] = \sum_{i=1}^m \mathbb{I}[y_j \in Y_i] \cdot \mathbb{I}[\psi_j(|\mathbf{x}_i\rangle) = r] \quad (0 \leq r \leq k), \quad (8)$$

and

$$\bar{\varsigma}_j[r] = \sum_{i=1}^m \mathbb{I}[y_j \notin Y_i] \cdot \mathbb{I}[\psi_j(|\mathbf{x}_i\rangle) = r] \quad (0 \leq r \leq k), \quad (9)$$

where

$$\psi_j(|\mathbf{x}_i\rangle) = \sum_{(|x^*>, Y^*) \in \mathcal{N}(|\mathbf{x}_i\rangle)} \mathbb{I}[y_j \in Y^*]. \quad (10)$$

$\psi_j(|\mathbf{x}_i\rangle)$ counts the number of neighbors that belong to category y_j in k nearest neighbors of the i -th coherent state. Correspondingly, $\varsigma_j[r]$ counts the number of coherent states that belong to category y_j themselves and exactly have r neighbors which belong to category y_j in k neighbors, while $\bar{\varsigma}_j[r]$ counts the number of coherent states that does not belong to category y_j and exactly have r neighbors which belong to category y_j in k neighbors. Consequently, the conditional probabilities in Eq. (5) can be calculated by

$$\mathbb{P}(C_j | H_j) = \frac{s + \varsigma_j[C_j]}{s \times (k + 1) + \sum_{r=0}^k \varsigma_j[r]}, \quad (11)$$

and

$$\mathbb{P}(C_j | \bar{H}_j) = \frac{s + \bar{\varsigma}_j[C_j]}{s \times (k + 1) + \sum_{r=0}^k \bar{\varsigma}_j[r]}, \quad (12)$$

where $1 \leq j \leq l$ and $0 \leq C_j \leq k$. Finally, a well-behaved quantum multi-label classifier $h(|\mathbf{x}\rangle)$ is obtained by the successful state learning.

Comparing with state-discrimination detector reported by our previous work [35], the proposed QMLC algorithm has several advantages. The most obvious merit is that QMLC has the ability to address the model of multi-label learning, thereby it is suitable to the high dimensional modulation strategy. In essence, QMLC belongs a part of data-processing in ML-CVQKD, so that it can be ran without any extra device or component. Moreover, the proposed ML-CVQKD with QMLC can further improve system's performance, we give the detailed analysis in next section.

IV. PERFORMANCE ANALYSIS

Before illustrating the detailed performance analysis of the QMLC-embedded ML-CVQKD system, it is necessary to present all input data since the proposed protocol is quite different from the traditional GG02 protocol.

As known, quantum channel of the fiber-based one-way quantum key distribution can be deemed a mapping function which can be described as [45]

$$q' = \sqrt{\eta}(q \cos \varphi_0 + p \sin \varphi_0) + \varepsilon, \quad (13)$$

$$p' = \sqrt{\eta}(p \cos \varphi_0 - q \sin \varphi_0) + \varepsilon, \quad (14)$$

where $\varphi_0 = |\theta - \theta'|$ is the phase drift during transmission and ε is Gaussian $(0, N_0 + \eta\epsilon)$ distribution. Fig. 6 shows 10^4 data points of eight-state modulated coherent state in phase space after passing 20km fiber-based quantum channel. Due to the impact of channel loss and noise, the transmitted states are distributed in phase space with a certain probability distribution. As can be seen, however, these chaotic points are hardly distinguished and their format cannot be directly used as input data for QMLC. We subsequently plot eight reference states and calculate the distance between each data point and each reference state. As a result, the original data points are mapped into eight-dimensional vector. Fig. 7 shows a part of 10^4 data points after extracting their distance features, each line represents a feature vector of each data point. We find that most distance values of feature vectors are located range from 0 to 9.5, while a few feature vectors contains high distance values. These high-value feature vectors are corresponding to the edge outliers in Fig. 6, which leads to performance reduction. To obtain better performance, we put forward a threshold function to filter the high-value feature vectors. As shown in Fig. 7, feature vectors which feature value beyonds black line should be discarded for performance improvement.

Different from the traditional CVQKD protocols, our protocol takes advantage of machine learning-based method to predict the unlabeled signal state, so that the traditional information theory-based metrics used in GG02 cannot precisely and comprehensively estimate the performance of our protocol. Hence, several machine learning criteria need to be introduced.

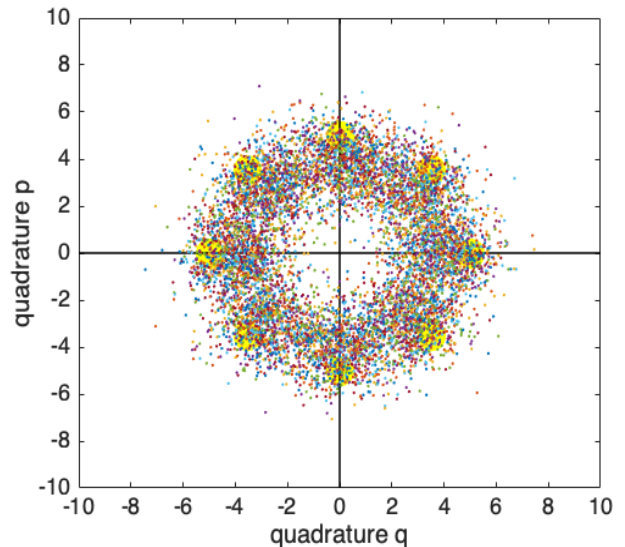


FIG. 6. 10^4 data points (colored) of eight-state modulated coherent state in phase space after passing 20km quantum channel. Yellow dots denote reference states. Modulation variance $V_m = 50$ and excess noise $\epsilon = 0.01$.

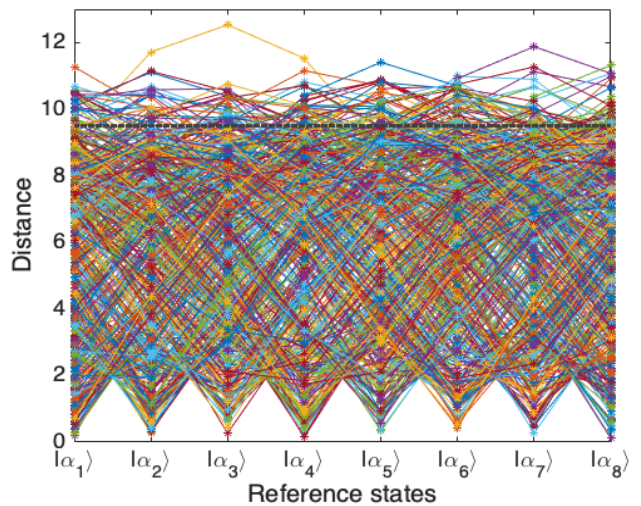


FIG. 7. Feature vectors of data points after extracting eight-dimensional distance values. Black dashed line represents filter threshold function.

Assuming there are three datasets, i.e., dataset A denotes samples which predicted as positive, dataset B denotes all positive samples, and dataset C denotes all samples. Fig. 8 shows the relationship between these datasets and their corresponding criteria, which are listed below.

Precision (Prec) describes the rate of positive samples in the samples which predicted as positive.

Recall (Rec) describes the rate of samples which predicted as positive in all positive samples.

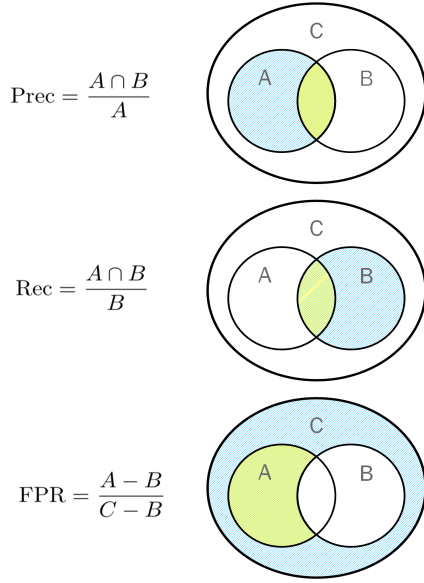


FIG. 8. The relationship of different datasets and their corresponding criteria.

False Positive Rate (FPR) describes the rate of samples which predicted as positive in all negative samples.

Actually, besides the above-listed criteria, there may be other criteria used in machine learning to estimate the specific system. The reason why we select these three is that the primary concern of our protocol is the correctness of the coherent state classification. We need to know how accurate QMLC can be and how many misclassifications it occurs. In addition, since QMLC is designed for solving multi-label classification problem, we deploy another criterion called *Average Precision* (AP), which evaluates the average fraction of labels ranked above a particular label $y \in Y$ which are in Y . It can be expressed as

$$\text{AP} = \frac{1}{g} \sum_{i=1}^g \frac{1}{|Y_i|} \times \sum_{y \in Y_i} \frac{|\{y' | \text{rank}_f(|\mathbf{x}_i\rangle, y') \leq \text{rank}_f(|\mathbf{x}_i\rangle, y), y' \in Y_i\}|}{\text{rank}_f(|\mathbf{x}_i\rangle, y)}, \quad (15)$$

where g is the number of data in testing set and $\text{rank}_f(\cdot, \cdot)$ is ranking function related to labels [41]. The performance improves with the increased AP, and the maximum perfect value is $\text{AP} = 1$.

Fig. 9 shows the performance of the QMLC-embedded ML-CVQKD system in terms of precision (a), recall (b), false positive rate (c) and average precision (d). According to the plots (a), (b) and (d), the performance of Prec/Rec/AP show the similar trend. Namely, it increases with the enlarged modulation variance and decreases with the risen channel loss. More specifically, the optimal performance can be achieved in both Prec and Rec when $V_m \geq 40$ regulated at a certain channel loss range. It illustrates that the QMLC-embedded ML-

CVQKD has the ability to accurately predict unlabeled positive signal states. In the meanwhile, plot (d) shows that the AP has larger range of perfect performance area. It illustrates that our protocol is well qualified for handling the multi-label classification problem of CVQKD. On the other hand, plot (c) shows the reduced FPR, and it illustrates that the level of misclassification of our protocol is well acceptable.

Although Prec/Rec/FPR/AP have shown the respective performance from different aspects, we still hope that one can use a metric to check the overall quality of the embedded QMLC. Therefore, *Receiver Operating Characteristic Curve* (ROC) [46], which describes the true positive rate of a certain classifier as a function of its FPR, is introduced. With ROC curve, one can explicitly tell the quality of the classifier: the curve more close to point (0,1), the performance better. Fig. 10 shows the ROC curves of QMLC. The gray line is the result of random guess, which illustrates that there is no performance improvement without using any classifier. For each label, however, the ROC curve is close to point (0,1) with embedded QMLC, which means the proposed classifier can dramatically improve the prediction performance of ML-CVQKD. We further calculate the *Area Under Curve* (AUC) for each label and thus obtain AUC value, which is a probability value range from 0 to 1. As a numerical value, AUC can be directly used for evaluating the quality of classifier. Therefore, the efficiency of quantum classifier Λ can be described by its AUC value, namely $\Lambda = \text{Average AUC}$ in our case. Moreover, a threshold range from 0.5 to 1 can be set to monitor the effectiveness of classifier. The state learning process must be interrupted and restarted if AUC value of current trained classifier less than a certain threshold.

Actually, the modulation variance is one of the crucial parameters impacting the performance of CVQKD system. However, the modulation variance V_m of the traditional eight-state modulated CVQKD cannot be set large value according to our previous work [42] in which the optimal $V_m = 0.3@100\text{km}$. Indeed, small modulation variance is usually required for the discretely-modulated CVQKD protocol as it is the only way to prevent information from being eavesdropped by Eve [7]. In the proposed ML-CVQKD protocol, fortunately, this problem can be well solved due to the usage of the machine learning framework. As known in the discrete modulation scheme, Eve can intercept modulated coherent states and resend them to Bob without introducing any noise if the modulation variance is large enough. The reason is that the encoding rule of discrete modulation is public for all users, so that Eve can precisely recover the information carried by their intercepted coherent states. For the proposed protocol, however, only Alice knows the encoding rule at the beginning, and Bob will learn the rule at the end of state learning process. Therefore, even Eve intercept the modulated coherent states, she cannot exactly recover information without knowing any encoding rule. Even if encoding rule is compromised somehow,

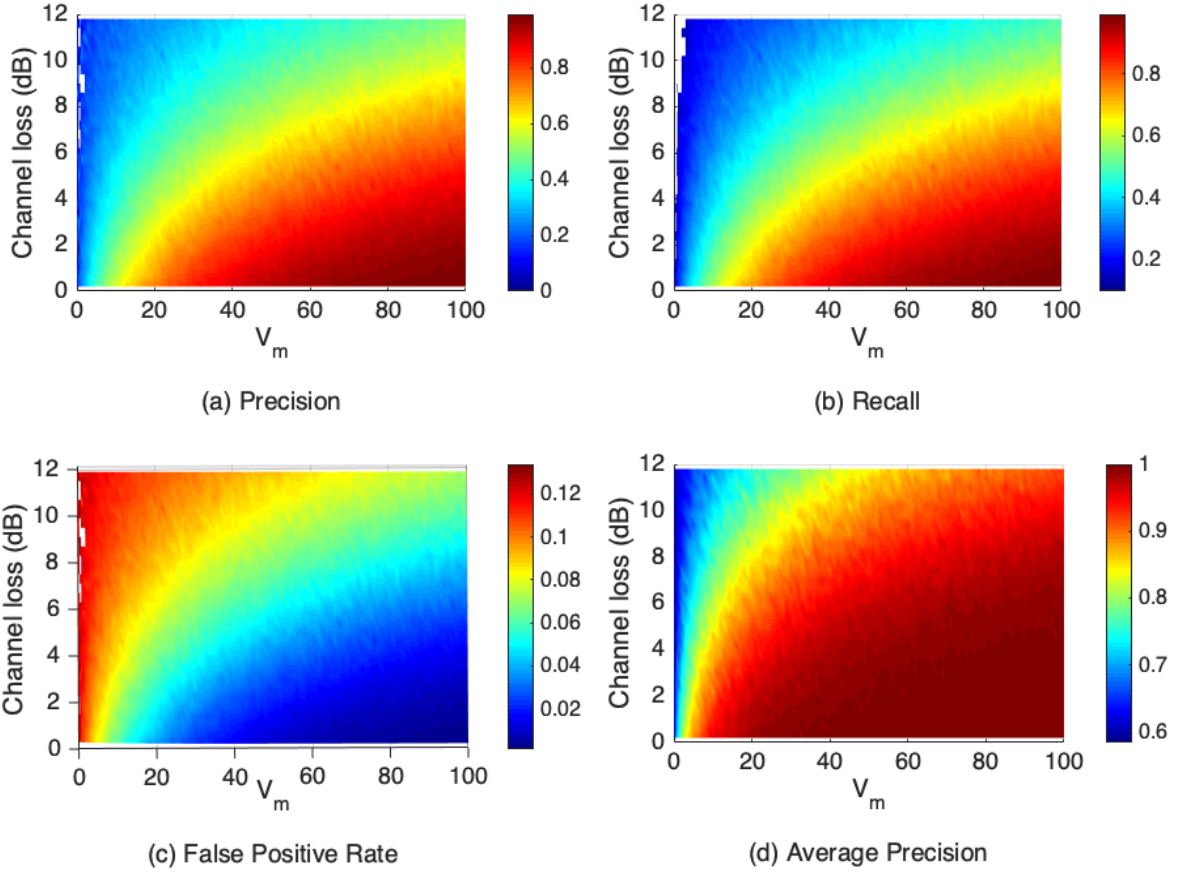


FIG. 9. Performance of the QMLC-embedded ML-CVQKD system in terms of (a) Precision, (b) Recall, (c) FPR and (d) Average Precision. The number of nearest neighbors is $k = 9$ and excess noise is $\epsilon = 0.01$. The training set contains 5000 data points and the testing set contains 10^4 data points.

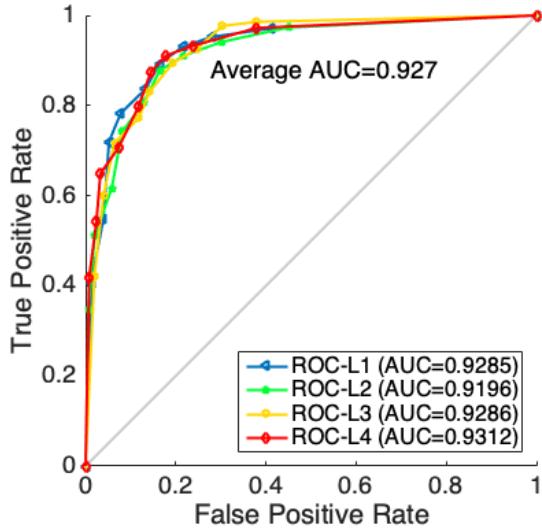


FIG. 10. ROC curves with respective AUC values of embedded quantum multi-label classifier. Gray line denotes the performance of random guess.

Alice and Bob can share a new encoding rule by restarting the state learning process. Therefore, the security of our protocol can still be guaranteed even if modulation variance is large.

Till now, we have demonstrated the performance of QMLC-embedded ML-CVQKD protocol in terms of machine learning-based metrics and thereby have shown its advantages. However, we still want to present a performance comparison for ML-CVQKD in traditional way so that researchers who do not familiar with machine learning can immediately evaluate how much improvement of the proposed protocol can be. As known in finite-size scenario, the secret key rate of the traditional CVQKD is given by [39]

$$K_{\text{fini}} = \frac{n}{N} [\beta I(A : B) - S_{\epsilon_{PE}}(E : B) - \Delta(n)], \quad (16)$$

where β is the efficiency for reverse reconciliation and $I(A : B)$ is the Shannon mutual information between Alice and Bob. The value N denotes the total number of the exchanged signals and n denotes the number of signals that is used for sharing key between Alice and Bob. The remained $m = N - n$ signals is used for parameter

estimation with failure probability is ϵ_{PE} . The parameter $S_{\epsilon_{PE}}(E : B)$ represents the Holevo bound [47] of the mutual information between Eve and Bob and needs to be calculated in parameter estimation. The parameter $\Delta(n)$ is related to the security of the privacy amplification, which is given by

$$\Delta(n) = (2\dim\mathcal{H}_B + 3)\sqrt{\frac{\log_2(2/\bar{\epsilon})}{n}} + \frac{2}{n}\log_2(1/\epsilon_{PA}), \quad (17)$$

where $\bar{\epsilon}$ is a smoothing parameter, ϵ_{PA} is the failure probability of privacy amplification, and \mathcal{H}_B is the Hilbert space corresponding to the Bob's raw key. Since the raw key is usually encoded on binary bits, we have $\dim\mathcal{H}_B = 2$. However, Eq.16 cannot be directly used to describe the finite-size performance of ML-CVQKD due to the data processing is quite different. First, nearly all raw key can be used for generating final secret key rather than sacrificing part of them for parameter estimation so that $\frac{n}{M}$ is approach to 1. Second, reconciliation including error correction is no longer required in ML-CVQKD since its duty is taken over by the embedded quantum classifier, so that reconciliation efficiency β is replaced by Λ . Therefore, the finite-size secret key rate for QMLC-embedded ML-CVQKD protocol can be expressed as

$$K_{\text{fini}}^{\text{ML}} = \Lambda_{\text{QMLC}} I(A : B) - \chi_E^{\text{ML}} - \Delta(n). \quad (18)$$

It is worthy noticing that term $S_{\epsilon_{PE}}(E : B)$ in Eq.16 is substituted by term χ_E^{ML} , which denotes the useful information Eve acquired by interacting with the quantum states during state prediction procedure. As shown in Tab.I, the encoding rule in discretely-modulated CVQKD is fixed and public, while it can be changed in ML-CVQKD by restart state learning procedure and only known by Alice at first. For example, Tab.II shows the decoding results caused by different encoding rules depicted in Tab.I. Assuming Alice randomly sends $|\alpha_3\rangle$, $|\alpha_6\rangle$ and $|\alpha_1\rangle$ to Bob, and Eve has the ability to totally intercept and resend these signal states without introducing any noise. For eight-state modulated CVQKD, Eve can precisely recover secret key according to the public encoding rule 1 (Alice, Bob and Eve share an identical secret key 001110001). For the proposed ML-CVQKD protocol, Eve cannot correctly decode secret key from intercepted states since only Alice and Bob know the encoding rule 2 after state learning 1 (Alice and Bob share an identical secret key 100001110, while Eve obtains a false secret key 011110001 if she decodes with public encoding rule 1). Even if encoding rule 2 is compromised, a new encoding rule 3 can be generated by restarting state learning procedure 2. As a result, Eve still cannot obtain the correct secret key (Alice and Bob share an identical secret key 1101110101, while Eve obtains a false secret key 100001110 if she decodes with compromised encoding rule 2). Moreover, the encoding length of ML-CVQKD is variable and, theoretically, it can be set to arbitrary length just as shown in encoding rule 3. Therefore, Eve become more difficult to obtain correct secret key from

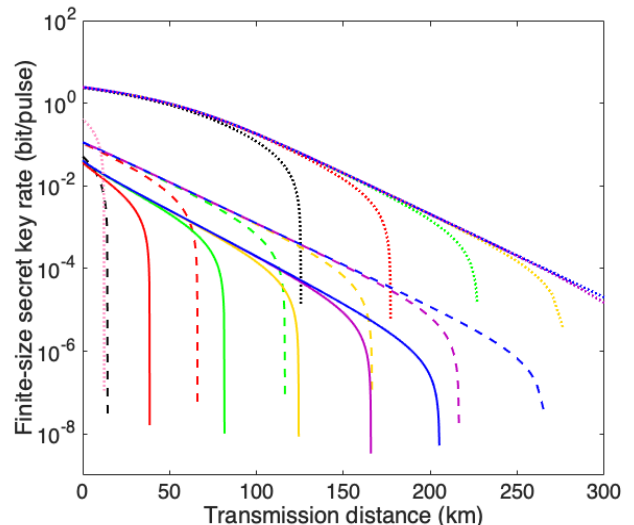


FIG. 11. Finite-size secret key rate as a function of transmission distance. Solid lines denote traditional eight-state CVQKD protocol with modulation variance $V_m=0.3$ [42], dashed lines and dotted lines represent the proposed ML-CVQKD with $V_m=0.3$ and $V_m=50$ respectively. From left to right, the colors correspond to block lengths of 10^3 (pink), 10^6 (black), 10^8 (red), 10^{10} (green), 10^{12} (yellow), 10^{14} (purple), 10^{16} (blue).

its intercepted states in ML-CVQKD.

Finally, fig.11 shows the finite-size performance of the proposed ML-CVQKD comparing with traditional eight-state CVQKD protocol. The result shows various advantages of the proposed protocol. First of all, both maximum transmission distance and secret key rate are improved, which makes ML-CVQKD more suitable for both high-speed and long-distance transmission situation. Moreover, since small variance is no longer required for the security of ML-CVQKD, the performance of ML-CVQKD can be further increased with the increase of modulation variance. Secondly, as can be seen from the pink dotted line and black dashed line, ML-CVQKD still can generate positive secret key when the block length is $10^3@V_m = 50$ and $10^6@V_m = 0.3$ respectively, while the minimum block length of traditional eight-state CVQKD for generating positive secret key is $10^8@V_m = 0.3$. This merit benefits to reducing computing and storing resource which makes ML-CVQKD better meets the need of real-time transmission. Note that Fig. 11 is a comparison which shows the upper bound of our protocol, a rigorous security proof is still needed for ML-CVQKD protocol, we leave this part to future study.

V. CONCLUSION

We have proposed a brand-new QMLC-embedded ML-CVQKD protocol, aiming to break the limitation of traditional pattern in CVQKD and establish a cross re-

TABLE I. Encoding rules in different scenarios.

| | $ \alpha_0\rangle$ | $ \alpha_1\rangle$ | $ \alpha_2\rangle$ | $ \alpha_3\rangle$ | $ \alpha_4\rangle$ | $ \alpha_5\rangle$ | $ \alpha_6\rangle$ | $ \alpha_7\rangle$ |
|--|--------------------|--------------------|--------------------|--------------------|--------------------|--------------------|--------------------|--------------------|
| Encoding rule 1: Eight-state modulated CVQKD (fixed, public) | 000 | 001 | 010 | 011 | 100 | 101 | 110 | 111 |
| Encoding rule 2: ML-CVQKD with state learning 1 (unfixed, private) | 111 | 110 | 101 | 100 | 011 | 010 | 001 | 000 |
| Encoding rule 3: ML-CVQKD with state learning 2 (unfixed, private) | 00 | 10101 | 11 | 1 | 1001 | 01 | 1011 | 101 |

TABLE II. Decoding results for Alice randomly sends $|\alpha_3\rangle$, $|\alpha_6\rangle$ and $|\alpha_1\rangle$ to Bob.

| | Alice | | | Eve | | | Bob | | |
|--|--------------------|--------------------|--------------------|--------------------|--------------------|--------------------|--------------------|--------------------|--------------------|
| | $ \alpha_3\rangle$ | $ \alpha_6\rangle$ | $ \alpha_1\rangle$ | $ \alpha_3\rangle$ | $ \alpha_6\rangle$ | $ \alpha_1\rangle$ | $ \alpha_3\rangle$ | $ \alpha_6\rangle$ | $ \alpha_1\rangle$ |
| Eight-state modulated CVQKD | 011 | 110 | 001 | 011 | 110 | 001 | 011 | 110 | 001 |
| ML-CVQKD after state learning 1 | 100 | 001 | 110 | 011 | 110 | 001 | 100 | 001 | 110 |
| ML-CVQKD after state learning 2 (encoding rule 1 is compromised) | 1 | 1011 | 10101 | 100 | 001 | 110 | 1 | 1011 | 10101 |

search platform between CVQKD and machine learning. A specialized quantum multi-label classification algorithm is elegantly designed as an embedded classifier for performance improvement of the ML-CVQKD system. The feature extraction for coherent state and machine learning-based criteria for ML-CVQKD are successively suggested. As a result, we have demonstrated a whole feasible process of the QMLC-embedded ML-CVQKD system with several potential characteristics. For example, the ability of tolerable excess noise and channel loss can be enhanced by taking advantage of the precise prediction, so that both secret key rate and transmission distance can be increased for the practical implementations. In addition, it waives the necessity of parameter estimation and error correction so that one can exploit more raw key to generate the final secret key, enabling in the high-rate CVQKD system. Moreover, the

quality of the whole system can be assessed by a single machine learning parameter so that the complicated estimation of covariance matrix of quantum system is no longer required. The size of data block used for correctly predicting unlabeled signal states is much less so that it is more suitable for real-time transmission. Besides, the QMLC-embedded ML-CVQKD protocol can be applied to the existing practical system without deploying any extra equipment.

ACKNOWLEDGMENTS

Q. Liao would like to thank Prof. X. Wang and Dr. T. Wang for the helpful discussions. This work is supported by the National Natural Science Foundation of China (Grants Nos. 61572529, 61871407) and the Fundamental Research Funds for the Central Universities.

-
- [1] C. H. Bennett and G. Brassard, in *Proc. IEEE International Conference on Computers Systems and Signal Processing* (1984) pp. 175–179.
- [2] S. Pirandola, U. L. Andersen, L. Banchi, M. Berta, D. Bunandar, R. Colbeck, D. Englund, T. Gehring, C. Lupo, C. Ottaviani, J. Pereira, M. Razavi, J. S. Shaari, M. Tomamichel, V. C. Usenko, G. Vallone, P. Villoresi, and P. Wallden, arXiv:1906.01645 (2019).
- [3] S. Takeda, M. Fuwa, P. van Loock, and A. Furusawa, *Phys. Rev. Lett.* **114**, 100501 (2015).
- [4] M. Gessner, L. Pezzè, and A. Smerzi, *Phys. Rev. A* **94**, 020101 (2016).
- [5] F. Grosshans, *Phys. Rev. Lett.* **94**, 020504 (2005).
- [6] M. Navascués and A. Acín, *Phys. Rev. Lett.* **94**, 020505 (2005).
- [7] A. Leverrier and P. Grangier, *Phys. Rev. Lett.* **102**, 180504 (2009).
- [8] A. Leverrier and P. Grangier, *Phys. Rev. A* **83**, 042312 (2011).
- [9] F. Furrer, T. Franz, M. Berta, A. Leverrier, V. B. Scholz, M. Tomamichel, and R. F. Werner, *Phys. Rev. Lett.* **109**, 100502 (2012).
- [10] A. Leverrier, R. García-Patrón, R. Renner, and N. J. Cerf, *Phys. Rev. Lett.* **110**, 030502 (2013).
- [11] A. Leverrier, *Phys. Rev. Lett.* **114**, 070501 (2015).
- [12] A. M. Lance, T. Symul, V. Sharma, C. Weedbrook, T. C. Ralph, and P. K. Lam, *Phys. Rev. Lett.* **95**, 180503 (2005).
- [13] X.-C. Ma, S.-H. Sun, M.-S. Jiang, M. Gui, and L.-M. Liang, *Phys. Rev. A* **89**, 042335 (2014).
- [14] S. Ghorai, P. Grangier, E. Diamanti, and A. Leverrier, arXiv (2019).
- [15] D.-X. Chen, P. Zhang, H.-R. Li, H. Gao, and F.-L. Li, *Quantum Information Processing* **15**, 881 (2016).
- [16] P. Huang, J. Fang, and G. Zeng, *Phys. Rev. A* **89**, 042330 (2014).
- [17] H. Zhang, J. Fang, and G. He, *Phys. Rev. A* **86**, 022338 (2012).
- [18] R. García-Patrón and N. J. Cerf, *Phys. Rev. Lett.* **97**, 190503 (2006).
- [19] F. Grosshans and P. Grangier, *Physical Review Letters* **88** (2002).
- [20] Q. Liao, Y. Guo, Y. Wang, and D. Huang, *Optics Express* **26** (2018).
- [21] S. Pirandola, C. Ottaviani, G. Spedalieri, C. Weedbrook, S. L. Braunstein, S. Lloyd, T. Gehring, C. S. Jacobsen, and U. L. Andersen, *Nat. Photon.* **9**, 397 (2015).
- [22] Z. Li, Y.-C. Zhang, F. Xu, X. Peng, and H. Guo, *Phys. Rev. A* **89**, 052301 (2014).

- [23] Y. Guo, Q. Liao, D. Huang, and G. Zeng, *Physical Review A* **95**, 042326 (2017).
- [24] C. Lupo, C. Ottaviani, P. Papanastasiou, and S. Pirandola, *Phys. Rev. A* **97**, 052327 (2018).
- [25] Y. Choi, O. Kwon, M. Woo, K. Oh, S.-W. Han, Y.-S. Kim, and S. Moon, *Phys. Rev. A* **93** (2016).
- [26] D. Huang, P. Huang, T. Wang, H. Li, Y. Zhou, and G. Zeng, *Phys. Rev. A* **94** (2016).
- [27] V. C. Usenko and F. Grosshans, *Physical Review A* **92** (2015).
- [28] P. Wang, X. Wang, J. Li, and Y. Li, *Optics Express* **25**, 27995 (2017).
- [29] Q. Liao, Y. Guo, C. Xie, D. Huang, P. Huang, and G. Zeng, *Quantum Information Processing* **17**, 1 (2018).
- [30] C. Weedbrook, *Phys. Rev. A* **87**, 022308 (2013).
- [31] Y. Guo, Q. Liao, Y. Wang, D. Huang, P. Huang, and G. Zeng, *Phys. Rev. A* **95** (2017).
- [32] P. Papanastasiou, C. Lupo, C. Weedbrook, and S. Pirandola, *Phys. Rev. A* **98**, 012340 (2018).
- [33] P. Huang, J. Huang, Z. Zhang, and G. Zeng, *Phys. Rev. A* **97**, 042311 (2018).
- [34] C. Robert, *Chance* **27**, 62 (2014).
- [35] Q. Liao, Y. Guo, D. Huang, P. Huang, and G. Zeng, *New J. Phys.* **20** (2018).
- [36] W. Liu, P. Huang, J. Peng, J. Fan, and G. Zeng, *Physical Review A* **97** (2018).
- [37] G. Carneiro, *IEEE Transactions on Pattern Analysis and Machine Intelligence* **29**, 394 (2007).
- [38] F. Grosshans and P. Grangier, *Phys. Rev. Lett.* **88**, 057902 (2002).
- [39] A. Leverrier, F. Grosshans, and P. Grangier, *Phys. Rev. A* **81**, 062343 (2010).
- [40] X.-Q. Jiang, P. Huang, D. Huang, D. Lin, and G. Zeng, *Physical Review A* **95**, 022318 (2017).
- [41] M. L. Zhang and Z. H. Zhou, *Pattern Recognition* **40**, 2038 (2007).
- [42] Y. Guo, R. Li, Q. Liao, J. Zhou, and D. Huang, *Physics Letters A* **382**, 372 (2018).
- [43] D. Yoon, K. Cho, and J. Lee, in *Vehicular Technology Conference* (2000).
- [44] M. M. Deza and E. Deza, *Reference Reviews* **24**, 1 (2009).
- [45] B. Qi, L. L. Huang, L. Qian, and H. K. Lo, *Physical Review A* **76**, 400 (2007).
- [46] N. R. Cook, *Circulation* **115**, 928 (2007).
- [47] M. A. Nielsen and I. L. Chuang, *Quantum Computation and Quantum Information* (Cambridge University Press, 2000).